numbered segments. The phenotypic expression of insect segments appears to be the result of a balance between two types of pair-rule loci. There are apparently no genes that control the expression of single segments as such. Workers in the field of fruit fly genetics were surprised that the expression of monosegments was the result of the interaction of pair-rule genes. However, it is evident that this segmental pairing is merely another manifestation of the underlying diplomerous organization of uniramian arthropods.

The suggestion that the phenotypic expression of segments could be the result of heterochronies in the segmental duplication cycles (*12*) has important consequences. The question of limb phylogeny shifts from explaining how one morphology evolved into another, to understanding how the timing of duplication cycles affects a range of morphologies. This makes the evolutionary transition of one body plan into another more comprehensible in terms of apparent convergences, character reversals, and discontinuities.

It now appears that uniramians can be more firmly linked with biramous arthropods than ever before. Interestingly, some confirmation of the events postulated here may be emerging from new analyses of molecular data (*16*), wherein uniramians are placed as the first offshoot of a line of evolution leading to the biramous arthropods.

The fact that *Tesnusocaris*, a 310-million-year-old Coal Age animal, provides insights concerning events of arthropod evolution that must have happened 600 million years ago in the early Cambrian is not contradictory. We think that Cambrian fossils do exist that clearly seem to have a similar anatomical form (*8*), but previously have been misinterpreted. *Tesnusocaris* is at present merely the best known fossil with this form. That *Tesnusocaris*, as a missing link in arthropod evolution, is a remipede should not be too surprising. This merely seconds the arguments for remipedes being a sister group to all other crustaceans (*9*). Other investigators hold positions contrary to this view (*5*), although to date no concrete arguments have been put forth against remipedes being built on the most primitive of crustacean body plans.

In conclusion, the assumption of serial homology has been the central paradigm governing comparisons between the body plans of various groups of segmented metazoans. In fact, it would seem impossible to attempt analyses of arthropod body plans without it. In the absence of evidence to the contrary, the paradigm of serial homology seemed not only reasonable, but necessary—despite the fact that comparisons inevitably reveal gross inconsistencies. The paradigm of serial homology is an assumption, however, that is untested and may prove misleading. Now, evidence offers a different possibility.

We suggest that the evolutionary sequence from annelid-like origins, through an onychophoran-like ancestor, to diplopodous myriapod-like uniramians established the base of arthropod evolution from which evolved crustaceans and possibly other biramian groups. It seems that duplication cycles leading to segment pairing and eventual fusion are the unique derived feature of the Arthropoda as a whole and have been a central factor in the flexibility of body plan design that has made the arthropods conspicuously successful since the Cambrian explosion some 600 million years ago.

REFERENCES AND NOTES

1. D. E. G. Briggs and R. A. Fortey, *Science* **246**, 241 (1989).
2. A. P. Gupta, *Arthropod Phylogeny* (Van Nostrand Reinhold, New York, 1979).
3. D. T. Anderson, *Embryology and Phylogeny in Annelids and Arthropods* (Pergamon, New York, 1973); S. M Manton, *The Arthropoda* (Oxford Univ. Press, Oxford, 1977).
4. J. Kukalova-Peck, *Can. J. Zool.* **61**, 1618 (1983).
5. R. R. Hessler and W. A. Newman, *Fossils Strata* **4**, 437 (1975).
6. H. K. Brooks, *J. Paleontol.* **29**, 252 (1955).
7. F. R. Schram and M. J. Emerson, *Environ. Southwest* **515**, 16 (1986).
8. M. J. Emerson and F. R. Schram, *Proc. San Diego Soc. Nat. Hist.*, in press.
9. F. R. Schram, *Crustacea* (Oxford Univ. Press, New York, 1986).
10. ———, *Fieldiana Geol.* **12**, 235 (1969).
11. H. Scheffel, *Zool. Jahrb. Abt. Allg. Zool. Physiol. Tiere* **71**, 624 (1965).
12. A. Minelli and S. Bortoletto, *Biol. J. Linn. Soc. London* **33**, 323 (1987).
13. F. R. Schram and W. D. Rolfe, *J. Paleontol.* **56**, 1434 (1982).
14. C. Nüsslein-Volhard and E. Weischaus, *Nature* **287**, 795 (1980); M. P. Scott and P. H. O'Farrell, *Annu. Rev. Cell Biol.* **2**, 49 (1986).
15. S. M. Cohen, *Nature* **343**, 173 (1990).
16. J. A. Lake, *Proc. Nat. Acad. Sci.* **87**, 763 (1990).

17. We thank V. Foe for help in understanding insect developmental genetics.

26 March 1990; accepted 8 August 1990

Side Chain Contributions to the Stability of Alpha-Helical Structure in Peptides

PINGCHIANG C. LYU, MARK I. LIFF, LUIS A. MARKY, NEVILLE R. KALLENBACH

Short peptides that contain significant α-helical structure in aqueous solution allow the investigation of the role of amino acid side chains in stabilizing or destabilizing α-helix structure. A host-guest system of soluble synthetic peptides was designed that consisted of chains with the block sequence $TyrSerGlu_4Lys_4X_3Glu_4Lys_4$, denoted EXK, in which X represents any "guest" amino acid residue. Circular dichroism spectroscopy indicates that the extent of helicity of these peptides follows the order Ala > Leu > Met > Gln > Ile > Val > Ser > Thr > Asn > Gly. This order differs from both host-guest copolymer values (Met > Ile > Leu > Ala > Gln > Val > Thr > Asn > Ser > Gly) and the tendencies of these amino acids to occur in helices in globular proteins (Ala > Met > Leu > Gln > Ile > Val > Asn, Thr > Ser > Gly), but matches the order found in a series of synthetic coiled-coil α helices, except for Ser. Proton nuclear magnetic resonance analysis of several EXK peptides indicates that these peptides are partially helical, with the helical residues favoring the amino terminus.

ABOUT ONE THIRD OF THE RESIDUES in globular proteins of known structure are estimated to be α helical in conformation (*1*). The reasons for this are imperfectly understood, although the question is of importance in trying to determine or predict how proteins fold. Chou and Fasman (*2, 3*) improved and extended a number of earlier, less complete statistical correlations to estimate the helical propensities of different side chains from the frequency of occurrence of amino acids in helical sequences in proteins of known structure. More current schemes seek to take longer range sequence correlations into account (*4*), but these entail fitting a much larger set of parameters than the simple Chou-Fasman version, comprehensive data for which are not yet available.

Scheraga and his co-workers (*5*) have done experiments to define the quantitative influence of each of the 20 standard side chains on the stability of α helices empirically, introducing the amino acid as a "guest" into a soluble copolymer of the form poly

Department of Chemistry, New York University, 4 Washington Place, New York, NY 10003.

(X,G*), where X denotes the guest amino acid and G* the "host" side chain, hydroxypropyl or hydroxybutyl glutamine. For each natural amino acid, a value of s, the equilibrium constant for adding that amino acid to the end of a nucleated helix (*6*), and an estimate of the effect of the amino acid on nucleating α helix, Zimm and Bragg's σ parameter, were reported (*5*). The results of this analysis showed an imperfect correlation with the probability values derived by Chou and Fasman (*2, 3*).

Subsequent investigations of helix stability in short natural and synthetic peptide fragments (*7–10*) revealed inconsistencies with these host-guest values. Many peptides of length 20 or less with helical structure have been found or synthesized, and temperature strongly influences their structure. Neither observation is consistent with predictions from host-guest experiments based on hydroxyalkyl glutamine host residues (*5*). It is thus necessary to reevaluate these parameters in different backgrounds and to establish whether a single, self-consistent set of values can be obtained for naturally occurring side chains. The relation between this set of values and values determined for α helices within globular proteins is of interest also. Site-directed sequence alterations in proteins make it possible to determine the differential free energy (ΔG) change for substituting amino acids at particular sites in proteins, including helical sequences (*11*). Whether or not the free energy differences in globular proteins are simply related to parameters determined from isolated helices in solution could prove crucial in understanding both the relative balance of forces in the two situations and how folding occurs.

Some factors that affect the structure and stability of isolated α helices have been identified. (i) The Ala side chain itself appears to exert a stronger stabilizing effect in short isolated α helices (*7–9*) than predicted by Chou-Fasman values, more complex schemes (*4*), or Scheraga's host-guest parameters (*5*). (ii) Charged groups can exert a direct influence on helix stability. The arrangement of positive and negative charges along a helix affects helix stability, seemingly by an interaction between charges and the helix dipole (*7, 12*). Side chains containing pairs of opposite charges spaced three residues apart so that they face each other on the surface of the helix can also form ion pairs (*9, 13*). (iii) The effect of the two natural side chains that destabilize α helix most effectively, Pro and Gly, can be rationalized in quite simple terms; Pro requires bending of the helix axis if it occurs in the interior of α helix, whereas Gly is thought to stabilize the coil form relative to helix more than other amino acids because of its greater

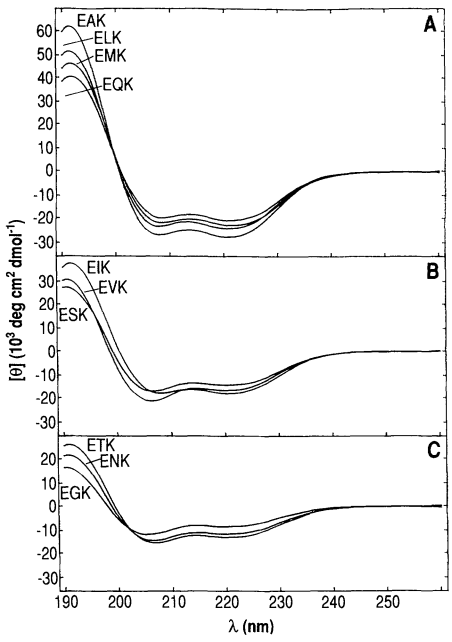

Fig. 1. CD spectra of ten peptides in 10 mM KF, neutral pH at 4°C (*19*). (**A**) Spectra of EAK, ELK, EMK, and EQK showing a well-defined isodichroic point near 201 nm. (**B**) Spectra of EIK, EVK, and ENK. No fixed isodichroic point is observed, and the minimum near 208 nm shifts to lower frequency. (**C**) Spectra of ETK, ENK, and EGK showing an isodichroic point near 203 nm. Peptides with high helix content shown in (A) appear to share common helix and coil characteristics, while those with medium helix content in (B) do not. Peptides with still lower helix content (C) again appear to have common helix and coil features different from those in (A).

conformational freedom in that state (*2, 14*). However, what distinguishes other side chains at different positions in a helix from those that are more or less stabilizing is not clear (*9, 15, 16*). Among chemically similar side chains, conformational restrictions imposed by helix formation are likely to be an important factor (*17*).

To approach this problem, consistent estimates of the helix-forming potential of each amino acid are needed in a background of natural rather than synthetic side chains. We have used a de novo designed peptide system that is highly soluble and shows partial intramolecular helix formation in aqueous solutions at low temperature to reevaluate the effects of different amino acid side chains on helix structure. The strategy is to introduce substitutions at internal sites of chains containing alternating blocks of Glu and Lys residues (*10, 18*)

succinyl-YSEEEEKKKKXXXEEEE-KKKK-NH_2

The succinyl group at the amino terminus and amidation of the carboxyl terminus have been found to promote helicity in short peptides (*7*). The alternation between acidic and basic side chains in these peptides permits ion pairing between E and K residues spaced at positions i, $i \pm 4$ along the chain near neutral pH, which also stabilizes α helix (*9*). Insertion of test side chains into the interior of this matrix enabled us to assess the effect on helicity of these residues in a relatively polar environment with minimal intermolecular effects. Initially we have chosen to substitute units consisting of three groups at a time to amplify potentially small differences among test side chains.

We recorded ultraviolet circular dichroism [CD (*19*)] spectra of ten synthetic peptides (*20*) of the EXK series: Ala (EAK), Leu (ELK), Met (EMK), Glu (EQK), Ile (EIK), Val (EVK), Ser (ESK), Thr (ETK), Asn (ENK), and Gly (EGK) as the X substituent in the sequence at 4°C and neutral pH, conditions that favor helix formation (*10*). The shape of these spectra, and in particular the value of the molar residue ellipticity, [θ], at 222 nm, provide a measure of the α helix content in simple polypeptides (*21*). Thus, the spectrum of EAK in Fig. 1 indicates a relatively high degree of helicity, that of EGK relatively little. Qualitatively, these values indicate that the relative order of effectiveness of side chains in stabilizing the α helix is A > L > M > Q > I > V > S > T > N > G. However, it is essential to establish that the helical structure in each peptide is intramolecular and not a consequence of the known tendency of α helices to associate intermolecularly. Two checks on this are shown in Fig. 2. In Fig. 2A, the dependence of [θ] at 222 nm on concentration is shown for the ten peptides at 4°C. No dependence on concentration is observed over the range studied. This result does not preclude a tight intermolecular interaction, however, such as occurs in coiled coils. A more stringent test of the molecularity of the helical structure is shown in Fig. 2B; as the helix in EAK unfolds with increasing temperature, the presence of an initial tight association at low temperature should be revealed as a dependence of the unfolding on peptide concentration (*22*). The concentration dependence of $[\theta]_{222}$ at four temperatures is shown for the unfolding of EAK, where it can be seen that the helix content estimated from the CD spectra shows no dependence on the peptide concentration at any point in the unfolding. We believe that the helix in these peptides is then intramolecular in origin and not intermolecular.

The order of effectiveness of different side chains that we observe is inconsistent with that found in either the host-guest experiments (*5*) or the frequencies of occurrence of these side chains in protein helices (*2, 3*) (Table 1). This order resembles that determined recently for five nonpolar side chains

Table 1. Helix content, free energy, and equilibrium constants for amino acid substitution in ten synthetic peptides relative to other scales.

Peptide	$-[\theta]_{222}$*	f†	$\Delta\Delta G_t$‡	$\Delta\Delta G_m$§	K_X‖	K_X/K_A¶	S_X/S_A#	$P_{\alpha X}/P_{\alpha A}$**
EAK	27,300	0.85	−0.52	−0.79	1.79	1.00	1.00	1.00
ELK	24,100	0.75	−0.40	−0.62	1.31	0.73	1.04	0.93
EMK	23,100	0.72	−0.38	−0.57	1.20	0.67	1.19	0.95
EQK	20,600	0.64	−0.31	−0.48	1.02	0.57	0.93	0.81
EIK	17,800	0.56	−0.25	−0.39	0.87	0.49	1.13	0.71
EVK	16,000	0.50	−0.20	−0.34	0.79	0.44	0.81	0.70
ESK	14,200	0.44	−0.16	−0.28	0.71	0.40	0.66	0.52
ETK	12,900	0.40	−0.13	−0.23	0.65	0.37	0.72	0.56
ENK	11,600	0.36	−0.10	−0.18	0.60	0.34	0.70	0.56
EGK	8,100	0.25	0	0	0.43	0.24	0.49	0.45

*Mean residue ellipticity (deg cm^2 dmol^{-1}) of the peptides at 222 nm (4°C, pH 7). Values are based on triplicate determinations with a standard deviation estimated to be less than ±3%. †$f = [([\theta]_{obs} - [\theta]_0)/([\theta]_{100} - [\theta]_0)]$, the fraction of helix; $[\theta]_0 = 0$ deg cm^2 dmol^{-1}, $[\theta]_{100} = -32{,}000$ deg cm^2 dmol^{-1} (*21*). ‡$\Delta\Delta G_t = (\Delta G_{EXK} - \Delta G_{EGK})/3$, on the basis of an all-or-none two-state model (*21*), where $\Delta G_{EXK} = -RT\ln[f/(1-f)]$. §The free energy of helix formation relative to Gly calculated from a multistate model (*28*) in which a helix sequence can exist at any possible sites in the chain (*6*). The actual ΔG value for Gly is +0.47 kcal/mol, so that Gln (or Q) is very nearly neutral with respect to the helix formation; those above Q are helix-stabilizing, those below it are destabilizing. ‖The equilibrium constant for helix formation, calculated from $\Delta\Delta G_m$. ¶Ratios of stability constants for helix formation of values in the previous column relative to Ala. For comparison, the ratio for A → G substitution in C-peptide (*7*) is 0.37 at 3°C on the basis of a two-state model; our value is 0.39 if based on a two-state calculation. #Ratios of s values for helix formation from copolymer host-guest experiments (*5*). **Ratios of normalized frequencies of occurrence (P_α) of amino acids in α helix in proteins (*2*).

by Baldwin's group (*9*); however, Leu in their peptides is found to be very close to Ala in its helix-forming ability, in marked contrast to our observation here. The order we observe is most consistent with that found by O'Neil and DeGrado (*16*), based on a complete series of substitutions at a solvent exposed site in a synthetic coiled-coil α-helical model. The single difference we find is Ser, which in ESK is less helix-stabilizing than Ile and Val, whereas in the dimer system (*16*) Ser is more stabilizing than the latter. The adjacent Ser residues in ESK may exert a cooperative destabilizing effect on helix structure (*23*), a hypothesis that can be tested by comparing a singly substituted sequence.

Free energy differences among amino acids in their effect on helical structure in this system can be calculated by assuming a model of the transition between helix and coil. One procedure that has been applied assumes helix formation is totally cooperative, hence that a given molecule is either fully helical or coil (*8, 9*). On the basis of such a "two-state" analysis, the difference between the free energy contribution of Ala to helix formation and that of Gly would be 0.52 kcal/mol, which is greater than that derived from host-guest copolymer experiments (*5*) or Chou-Fasman probabilities (*3*) (Table 1).

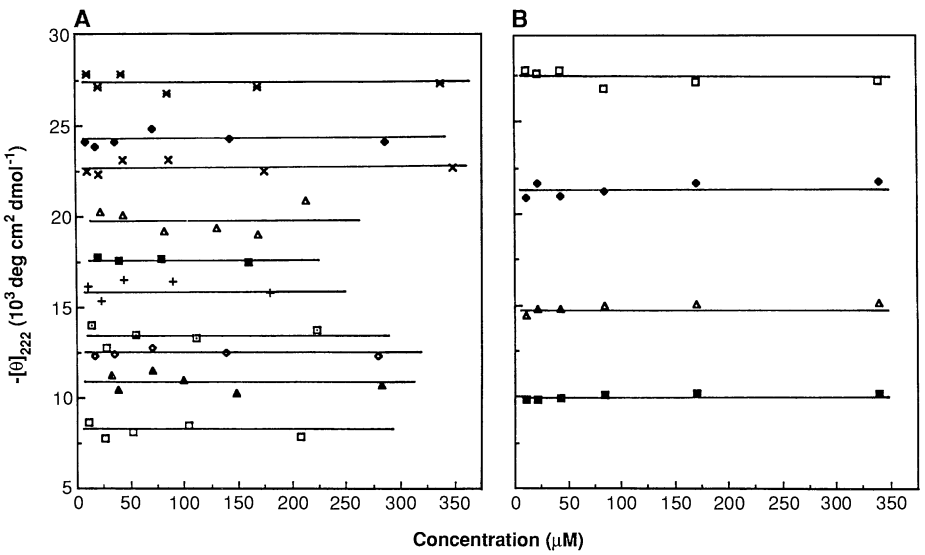

Fig. 2. Effect of concentration on the CD spectra of nine peptides. (**A**) Dependence of molar ellipticity per residue at 222 nm on concentration at 4°C of EAK (—**x**—), ELK (◆), EMK (**x**), EQK (△), EIK (■), EVK (+), ESK (⊡), ETK (◇), ENK (▲), and EGK (□) and (**B**) of EAK at 4°C (□), 25°C (◆), 50°C (△), and 75°C (■). All measurements were performed in 10 mM KF, neutral pH with a 1-mm pathlength cell. The lines shown are best-fit linear regression lines. Uncertainties in $[\theta]_{222}$ values are estimated to be ±2%, with most of the error being in the measurement of concentration rather than the CD measurement, which represents the average of at least three determinations [see (*19*)].

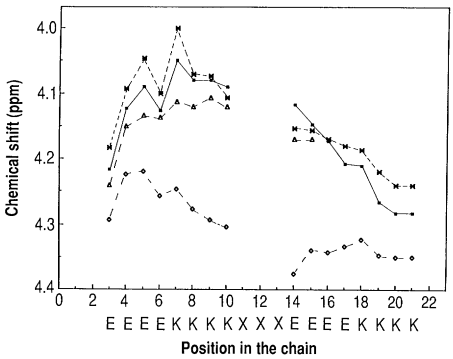

Fig. 3. The chemical shifts of the Cα protons at positions of identical sequence in four peptides, EAK (------); ELK (——); EK (·—·—·), the parent species lacking any insert; and EGK (—··—··). The data are derived from TOCSY experiments, run at 25°C with a mixing time (50 ms) and 5 mM concentration of peptide in each case. A statistical correlation between upfield shifts of these protons and helix content has been reported (*24, 27*). The other NMR criteria of helicity noted in the text reveal a similar distribution of helical residues in EAK, ELK, and EK. The Glu and Lys block toward the amino terminus from the substitution site has greater helical content than the corresponding block located at the carboxyl terminus in all peptides we have studied. The values of the CαH shifts for the maximally helical segment from residues 5 to 8 in the chain correlates well with the values of $[\theta]_{222}$ determined in CD experiments: EAK > ELK > EK > EGK. The uncertainty in chemical shift values is approximately ±0.01 ppm.

However, ^{1}H nuclear magnetic resonance (NMR) spectroscopy makes it possible to localize the helical structure within the chain quite precisely (*24*). We have investigated several of these peptides, including EAK, ELK, and EGK, by this method. Complete assignments of the spectra of these species have been achieved, despite the degeneracy in side chains, by use of a combination of total correlation spectroscopy (TOCSY) (*25*) and nuclear Overhauser and exchange spectroscopy (NOESY) (*26*) experiments. Several NMR criteria can distinguish helical segments from extended or coil regions (*24*), including NOEs indicating proximity between pairs of adjacent NH protons, NOEs between NH residues and the CαH three residues down the chain, the value of the three-bond coupling constants $^3J_{\alpha H}$, as well as the chemical shifts of the CαH protons (*27*). In contrast to the simplest hypothesis that chains are completely helix or coil, the helical structure within EAK, ELK, and the parent species is seen by these criteria to be nonuniformly distributed within each chain. The trend in CαH chemical shifts is illustrated in Fig. 3 as an example; upfield shifts of these protons correlate with α helicity (*24,*

27). The unsubstituted parent species has less α helix than EAK or ELK, while all of these are more helical than EGK. This order is consistent with that determined by CD spectroscopy (Table 1), and within each helical peptide there is a tendency for residues nearer the amino terminus to be helical, while those near the carboxyl terminus are less so.

A more realistic estimation of the differences in helicity among these molecules should account for the fact that a given chain can exist in partially helical, and partially coiled conformations, rather than a two-state situation. A statistical model (*6*), in which the helical sequence is allowed to occupy any positions in these short chains, allows us to calculate the multistate $\Delta\Delta G_m$ values (*28*). The relative order is seen to be preserved, while the free energy differences are seen to increase as a consequence of the presence of intermediate states. This analysis requires a value for σ, the equilibrium constant for helix initiation (*6*); in Table 1 we used 1×10^{-3} (*28*). However, these numbers are relatively insensitive to σ values from 2.5×10^{-3} to 1×10^{-4} (*5*). The agreement between the $\Delta\Delta G_m$ values at 4°C and those found by O'Neil and DeGrado at 25°C (*16*) is good.

The advantages of our system are that the peptides are short, soluble, and apparently monomeric at low concentrations. Since the parent chain lacking any X substitution is nearly 60% α helical, the role of each guest side chain on propagating rather than nucleating helical structure is emphasized; the differences between side chains should reflect differences in values of *s* rather than σ (*6*). Moreover, location of the substitution site at the center of the chains avoids helix "capping" effects (*15, 29*). While in principle any test residue can be evaluated by incorporating it in the cassette, side chains that are capable of interacting specifically with the flanking Glu and Lys blocks will yield estimates biased by these interactions. The role of next-neighbor sequence and position of test residues in the X block has been examined by comparing the helical structure in ELK and EGK with the substitution Leu-Gly-Leu (*30*); the helix content in this peptide matches that predicted from the appropriate average of those in ELK and EGK, which are triply substituted. Substitution of single residues in short alanine-rich helical peptides is effectively independent of position and additive (*8, 9*), supporting the hypothesis that a side chain exerts its effect on helix structure at a local level.

The results of this survey of ten EXK peptides reveal an order and quantitative *s* values consistent with those determined by O'Neil and DeGrado (*16*), with the exception of Ser, which we believe is likely to exhibit unusual behavior in clusters (*23*). Since the two systems are different, the extent of qualitative and quantitative agreement encourages us to anticipate that a single set of *s* values exists that describes α-helix formation under conditions including those representing early stages in folding nascent polypeptide chains. It is not unexpected that the order we observe differs from Chou-Fasman values (*2, 3*) and host-guest values (*5*). The former probabilities describe helical structures in globular proteins in which the balance of forces stabilizing individual helices is likely to differ from that governing folding of an isolated helix. At present, we do not understand the reasons for our disagreement with the results on the series of substituted Ala peptides studied in (*9*). The bulky Leu side chain may compete more effectively than the smaller Ala side chain with salt bridges that span the insertion site. However, the relative effects of Ile and Val seen in the two series are consistent, yet should show a comparable effect. Alternatively, the coil forms of the peptides in these two series might differ, altering the apparent *s* values. The order of side chain effectiveness and calculated free energy values reflect helix-coil differences, and characterizing the coil forms poses problems. The distinctive isodichroic behavior in EXK peptides with high, medium, and low helix content (Fig. 1) might in fact reflect differences among the coil states. To proceed further, details of the interactions present in both the helix and coil forms of these peptides need to be defined precisely.

REFERENCES AND NOTES

1. T. E. Creighton, *Proteins* (Freeman, New York, 1984).
2. P. Y. Chou and G. D. Fasman, *J. Mol. Biol.* **74**, 263 (1973); *Biochemistry* **13**, 211 (1974); *ibid.*, p. 222; *Adv. Enzymol.* **47**, 45 (1978); G. D. Fasman, in *Prediction of Protein Structure and the Principles of Protein Conformation*, G. D. Fasman, Ed. (Plenum, New York, 1989), pp. 193–316.
3. M. Levitt, *Biochemistry* **17**, 4277 (1978).
4. J. Garnier, D. J. Osguthorpe, B. Robson, *J. Mol. Biol.* **120**, 97 (1978); J.-F. Gibrat, J. Garnier, B. Robson, *ibid.* **198**, 425 (1987).
5. H. A. Scheraga, *Pure Appl. Chem.* **50**, 315 (1978); M. Sueki *et al.*, *Macromolecules* **17**, 148 (1984).
6. B. H. Zimm and W. K. Bragg, *J. Chem. Phys.* **31**, 526 (1959).
7. K. R. Shoemaker *et al.*, *Proc. Natl. Acad. Sci. U.S.A.* **82**, 2349 (1985); K. R. Shoemaker *et al.*, *Nature* **326**, 563 (1987); K. G. Strehlow and R. L. Baldwin, *Biochemistry* **28**, 2130 (1989).
8. G. Merutka and E. Stellwagen, *Biochemistry* **28**, 352 (1989); *ibid.* **29**, 894 (1990).
9. S. Marqusee and R. L. Baldwin, *Proc. Natl. Acad. Sci. U.S.A.* **84**, 8898 (1987); S. Marqusee, V. Robbins, R. L. Baldwin, *ibid.* **86**, 5286 (1989); S. Padmanabhan *et al.*, *Nature* **344**, 268 (1990).
10. P. C. Lyu, L. A. Marky, N. R. Kallenbach, *J. Am. Chem. Soc.* **111**, 2733 (1989); in *Peptides, Proceedings of the Eleventh American Peptide Symposium*, J. E. Rivier and G. R. Marshall, Eds. (ESCOM Science, Leiden, the Netherlands, 1990), pp. 632–634.
11. S. Dao-Bin, W. A. Baase, B. W. Mathews, *Proteins Struct. Funct. Genet.* **7**, 198 (1990).
12. W. G. J. Hol, *Prog. Biophys Mol. Biol.* **45**, 149 (1985).
13. D. J. Barlow and J. M. Thornton, *J. Mol Biol.* **168**, 867 (1983); M. Sundaralingam *et al.*, *Proteins Struct. Funct. Genet.* **2**, 64 (1987).
14. L. Piela, G. Nemethy, H. A. Scheraga, *Biopolymers* **26**, 1587 (1987). J. Hermans (private communication) has recently demonstrated the effects of Ala → Pro and Ala → Gly substitution in a dynamics calculation on short oligo Ala helices.
15. L. G. Presta and G. D. Rose, *Science* **240**, 1632 (1988); J. S. Richardson and D. C. Richardson, *ibid.*, p. 1648.
16. K. T. O'Neil and W. F. DeGrado, *ibid.* **250**, 646 (1990).
17. L. Piela, G. Nemethy, H. A. Scheraga, *Biopolymers* **26**, 1273 (1987); M. J. McGregor, S. A. Islam, M. J. E. Sternberg, *J. Mol. Biol.* **198**, 295 (1987).
18. The single-letter abbreviations for amino acids used are: A, Ala; E, Glu; G, Gly; I, Ile; K, Lys; L, Leu; M, Met; N, Asn; Q, Gln; S, Ser; T, Thr; V, Val; and Y, Tyr.
19. The CD spectra were recorded on an Aviv DS60 spectropolarimeter equipped with an HP Model 89100A temperature controller. The instrument was calibrated with (+)-10-camphorsulfonic acid [G. C. Chen and J. T. Yang, *Anal. Lett.* **10**, 1195 (1977)]. Measurements were carried out in 10 mM KF with 1-mm pathlength cells. The pH was adjusted with HCl and NaOH. The concentrations in CD experiments were 25 to 40 μM, except during the determination of concentration dependence.
20. Peptides were synthesized (MilliGen/Biosearch 9600 automated solid-state synthesizer) with the use of F-moc (fluorenyl methoxycarbonyl) chemistry. Benzotriazolyloxotris(dimethylamino)phosphonium hexafluorophosphate (BOP), in conjunction with 1-hydroxybenzotriazole (HOBT), was used as coupling reagent. Peptides were cleaved from the resin in 70% trifluoroacetic acid, 25% dichloromethane, and 5% dimethyl sulfide at room temperature for 2 hours. All peptides were amidated at the COOH-terminus by use of MilliGen/Biosearch peptide amide linker (PAL) resin and succinylated at NH_2-terminal by succinic anhydride in dimethyl formamide containing an equivalent of triethylamine to favor charge interactions with the helix dipole (*12*). Peptides were purified on a reversed-phase Deltapack C18 high-performance liquid chromatography (HPLC) column (Waters) with a gradient of 0 to 30% acetonitrile in 0.1% trifluoroacetic acid. The detector was set at 270 nm to take advantage of the presence of the Tyr residue at N1 position. Incorporating this Tyr residue not only facilitates purification of the product but also makes it possible to determine the peptide concentration accurately from the extinction coefficient of this side chain in 6 M guanidine HCl [J. F. Brandts and L. J. Kaplan, *Biochemistry* **12**, 2011 (1973)]. Each peptide was desalted on a Sephadex G-10 column and checked for purity by analytic HPLC. The correct primary ion molecular weights of the purified products were confirmed by fast-bombardment mass spectrometry (FAB-MS, M-Scan, Inc., West Chester, PA).
21. N. Greenfield and G. D. Fasman, *Biochemistry* **8**, 4108 (1969). Relative free energies of helix formation can be estimated roughly by converting CD spectra to a scale of helix content, on the basis of an all-or-none equilibrium between helix and coil "states": H ⇔ C, with equilibrium constant K_h. In the notation of Zimm and Bragg (*6*), $K_h = \sigma\Pi s_i$, where σ is the nucleation constant and each side chain, i contributes a factor $s_i = \exp(-\Delta G_i/RT)$ to the equilibrium constant of the helix, where ΔG_i is the corresponding free energy change, R the gas constant, and T absolute temperature. The overall fractional helicity (f) is estimated from the molar residue ellipticity at 222 or at 208 nm: $f = ([\theta]_{obs} - [\theta]_0)/([\theta]_{100} - [\theta]_0)$. The value of the molar ellipticity per residue (−32,000 deg cm^2 dmol^{-1}) corresponding to 100% helix was obtained by TFE titration (*9*) of peptide EAK. The corresponding value of $[\theta]_0$ (0 deg cm^2 dmol^{-1}) was determined by

an analogous experiment by using a denaturant, guanidine hydrochloride, with the peptides EAK, ELK, and EGK at different temperatures. The two-state equilibrium constant for the helix-coil transition is $K_h = f/(1 - f)$.
22. S. P. Ho and W. F. DeGrado, *J. Am. Chem. Soc.* **109**, 6751 (1987).
23. P. S. Kim and R. L. Baldwin, *Nature* **307**, 329 (1984); J. W. Nelson and N. R. Kallenbach, *Biochemistry* **28**, 5256 (1989).
24. A summary of methods is given in K. Wüthrich, *NMR of Proteins and Nucleic Acids* (Wiley, New York, 1986), p. 166. Data on the EXK peptides are from M. I. Liff, P. C. Lyu, N. R. Kallenbach, *Polym. Prepr.* **31**, 139 (1990), and unpublished results.
25. D. G. Davis and A. Bax, *J. Am. Chem. Soc.* **107**, 2820 (1985).
26. A. Kumar, R. R. Ernst, K. Wüthrich, *Biochem. Biophys. Res. Commun.* **95**, 1 (1980).
27. L. Szilagyi and O. Jardetzky, *J. Magn. Reson.* **83**, 441 (1989).
28. This model is equivalent to expanding the Zimm-Bragg (*6*) partition function in the limit of single helical sequences in short chains, retaining terms that are linear in σ, taken to be 1×10^{-3} [based on experimental data on Lys polymers, T. V. Barskaya and O. B. Ptitsyn, *Biopolymers* **10**, 2181 (1971), as well as the mean value from theoretical calculations by A. Englert *et al.*, *Macromolecules* **8**, 655 (1975)]. With the additional factor that the CD signal for a helix varies with the number of helical residues [we use the approximation that for a helix of k residues, $[\theta(k)]_{222} = [\theta]_{100}(1 - 1/k)$], the value of $[\theta]_{222}$ for any given chain can be calculated if the appropriate s values are known or can be estimated. The limiting values of $[\theta]_{100}$ and $[\theta]_0$ determined as described in (*21*) are also used for this calculation.
29. L. Serrano and A. R. Fersht, *Nature* **342**, 296 (1989); Ser was introduced at position 2 in the EXK peptides to provide a positive N capping effect.
30. P. C. Lyu, P. Wang, M. I. Liff, N. R. Kallenbach, unpublished results.
31. Supported by NIH grants GM 40746 and RR 02497 and NSF grants DIR 8722895 and DMB 84-13986. We thank W. F. DeGrado for sharing data and for helpful discussions.

4 May 1990; accepted 4 September 1990

Increased Activity of Calcium Leak Channels in Myotubes of Duchenne Human and *mdx* Mouse Origin

PEYING FONG, PAUL R. TURNER, WILFRED F. DENETCLAW, RICHARD A. STEINHARDT*

Elevated free Ca^{2+} concentrations found in adult dystrophic muscle fibers result in enhanced protein degradation. Since the difference in concentrations may reflect differences in entry, Ca^{2+} leak channels in cultures of normal and Duchenne human myotubes, and normal and *mdx* murine myotubes, have been identified and characterized. The open probability of leak channels is markedly increased in dystrophic myotubes. Other channel properties, such as mean open times, single channel conductance, ion selectivity, and behavior in the presence of pharmacological agents, were similar among myotube types. Compared to the Ca^{2+} concentrations in normal human and normal mouse myotubes, intracellular resting free Ca^{2+} concentrations ($[Ca^{2+}]_i$) in myotubes of Duchenne and *mdx* origin were significantly higher at a time when dystrophin is first expressed in normal tissue. Taken together, these findings suggest that the increased open probability of Ca^{2+} leak channels contributes to the elevated free intracellular Ca^{2+} concentration in Duchenne human and *mdx* mouse myotubes.

ADULT *mdx* SINGLE SKELETAL FIBERS have higher levels of intracellular free Ca^{2+} than normal mouse skeletal fibers; these elevated Ca^{2+} concentrations correlate with increased protein degradation rates in the dystrophic condition (*1*). The defective gene responsible for Duchenne muscular dystrophy in humans and the dystrophic condition of the *mdx* mouse results in the absence of dystrophin in muscle cells and brain tissue (*2–4*). Dystrophin is localized primarily to the sarcolemma of skeletal muscle fibers (*5, 6*). The dystrophin NH_2-terminal coding sequence is similar to that of α-actinin and may be involved in the anchorage of F-actin filaments to cell membranes (*7, 8*). Dystrophin is associated with the cell membrane by attachment to an integral membrane protein (*9, 10*). We hypothesized that the basic mechanism underlying the pathology of muscular dystrophy could involve the modulation of Ca^{2+} leak channels whose properties are altered by the absence of dystrophin.

Higher concentrations of free $[Ca^{2+}]_i$ measured in freshly dissected intact skeletal muscle fibers from mice, as well as in 3-week-old cultured human myotubes, correlated with the absence of dystrophin (*1, 11*). Before we could test any hypothesis of how $[Ca^{2+}]_i$ becomes elevated in dystrophic tissues, it was necessary to establish that the defect in Ca^{2+} regulation was present in the myotube stages being compared. Dystrophin expression is detectable after myoblast fusion and shows a predominantly sarcolemmal distribution within a few days of myotube formation (*12–14*). We therefore compared $[Ca^{2+}]_i$ in normal versus dystrophic myotubes from human and mouse 6 to 15 days after myoblast fusion. Resting $[Ca^{2+}]_i$ values for normal mouse and human myotubes were 82 ± 7 nM (mean ± SEM) (n = 45) and 55 ± 5 nM (n = 78), respectively (Fig. 1); the analogous values for myotubes from the *mdx* mouse and Duchenne human were already significantly elevated [110 ± 7 nM (n = 64) and 76 ± 5 nM (n = 78), respectively]. Exposure to a tenfold increase in extracellular Ca^{2+} (18 mM) showed $[Ca^{2+}]_i$ in normal mouse myotubes to be tightly regulated, whereas $[Ca^{2+}]_i$ rose dramatically in *mdx* myotubes (Fig. 1A). Unlike $[Ca^{2+}]_i$ in normal mouse myotubes, $[Ca^{2+}]_i$ in normal human myotubes increased under these conditions. However, the rate of increase of $[Ca^{2+}]_i$ was significantly higher in the Duchenne human myotubes (Fig. 1B). Thus, the ability to regulate free $[Ca^{2+}]_i$ was impaired in myo-

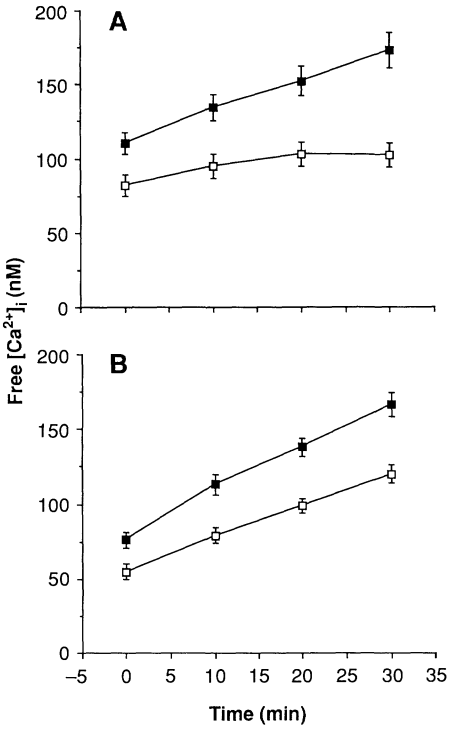

Fig. 1. Intracellular free Ca^{2+} estimated by fura 2 fluorescence in normal and dystrophic myotubes after a tenfold extracellular Ca^{2+} increase. (**A**) Normal mouse (□) and *mdx* mouse (■) myotubes and (**B**) normal human (□) and Duchenne human (■) myotubes. From 6 to 15 days after myoblast fusion, ratio images of myotubes were recorded over a 30-min period at the indicated time points (±1.5 min). At time 0, myotubes were bathed in a Ringer solution containing 1.8 mM extracellular Ca^{2+} (138 mM NaCl, 2.7 mM KCl, 1.8 mM $CaCl_2$, 1.06 mM $MgCl_2$, 12.4 mM Hepes, and 5.6 mM glucose, pH 7.2). Myotubes were then exposed to a Ringer solution containing 18.0 mM calcium. The mean $[Ca^{2+}]_i$ (nM ± SEM) is shown. Free Ca^{2+} was calculated as described (*21*).

Department of Molecular and Cell Biology, Division of Cell and Developmental Biology, University of California, Berkeley, CA 94720.

*To whom correspondence should be addressed.